Solar Energy 257 (2023) 314–323

Contents lists available at ScienceDirect

Solar Energy

journal homepage: www.elsevier.com/locate/solener

Fabrication of DSSC based on *Capsicum annuum* and *Tamarindus indica* plant seeds extract as natural photosensitizers

Nasim Sarwar [a], Monas Shahzad [b], Rabia Ghaffar [c], Khalid Javed [a], Mahroze Munam [a], Aneel Pervez [a], Abdul Ghaffar [d,*]

[a] Department of Physics, Forman Christian College (A Chartered University), Lahore 54600, Pakistan
[b] NanoScience Technology Center, University of Central Florida, USA
[c] Division of Science and Technology, Department of Botany, University of Education, Lahore 54000, Pakistan
[d] Department of Physics, Government College University, Lahore 54000 Pakistan

ARTICLE INFO

Keywords:
Natural dyes
DSSC
ZnO-based films
Graphite & PEDOT.PSS
J-V curves

ABSTRACT

Twelve dye-sensitized solar cells (DSSCs) were fabricated using *Capsicum annuum* and *Tamarindus indica* seeds extract as natural photosensitizing dyes. Zinc oxide-based three different films were employed as charge transporters, whereas graphite and PEDOT:PSS were adopted as electrode materials. The optical character of natural dyes and zinc oxide-based layers was obtained by UV–vis spectroscopy. Structural information was achieved by X-ray diffraction and modes of vibrations were obtained by Fourier Transform IR spectroscopy. Different schemes of DSSCs were considered by choosing from metal oxide films, seed extract, and electrode material. J-V curves recorded for all the DSSCs-configurations revealed that the maximum power conversion efficiency of 1.65% was found in the case of DSSC which comprised *Capsicum annuum* (dye), zinc oxide, and graphite as an electrode. Minimum 0.43% efficiency was obtained for the DSSC based on *Capsicum annuum* as a dye, Al-doped zinc oxide film, and PEDOT:PSS as an electrode. This study is a way forward to using recyclable natural resources for sustainable and economical solar power conversion devices.

1. Introduction

Various materials are being investigated to develop devices to address the challenges associated with energy generation. Dye-sensitized solar cells (DSSCs) are serving this purpose up to a certain extent. Photovoltaic cell (PVC) technology relies on organic and inorganic nanomaterials for its construction. A PVC connects the nanomaterials and electrodynamical nature of dyes to achieve the goals of solar energy conversion with possible maximum efficiency, sustainability, and reliability (Shalini et al., 2015).

DSSCs are photovoltaic devices that generate electrical energy from sunlight (El-Agez et al., 2014). They have been extensively explored since their beginning (O'Regan and Grätzel, 1991; Grätzel, 2001). Metal oxide-based dye-sensitized solar cells have been broadly studied to see the role of dye molecules in the sensitization of nanocrystalline structures. For the DSSCs synthesis, different semiconductor metal oxides, ZnO, TiO_2, Nb_2O_5, SnO_2, etc., are famous due to their low cost, high dielectric constant, and high refractive index. Moreover, these metal oxides are further co-doped with other metals for better performance by modifying structural and optical properties (Banerjee, 2011; Bazargan et al., 2011). The ZnO nanoparticles layer provides a high surface area, mesoporous structure, and an appropriate band gap of 3.7 eV. Specifically, zinc oxide has been an ideal alternative to TiO_2 because of a similar conduction band edge suitable for proper electron injection from excited dyes and also provides better electron transport due to its higher electronic mobility (Nukunudompanich et al., 2015; Ariyasinghe et al., 2013).

Solar cells based on ZnO nanomaterial are potentially favorable because of their easy construction, economical, and alternative to traditional photovoltaic devices. The efficiency and stability of DSSC using ZnO nanoparticles and dye-sensitized substances depend upon electron transport, dye absorption ability, band gap, and the nature of the semiconductor materials. Similarly, for large-scale production (Nukunudompanich et al., 2015; Ariyasinghe et al., 2013; Xu et al.,

Abbreviations: ZO, ZnO; AZO, Al-doped ZnO; NZO, Ni-doped ZnO; DSSC, dye-sensitized solar cell; FTO, fluorine-doped tin oxide; HSE, high stability electrolyte; FF, fill factor; FTIR, Fourier-transform infrared spectroscopy.

* Corresponding author.
E-mail address: abdulghaffar@gcu.edu.pk (A. Ghaffar).

https://doi.org/10.1016/j.solener.2023.04.039
Received 4 June 2022; Received in revised form 30 March 2023; Accepted 18 April 2023
Available online 29 April 2023

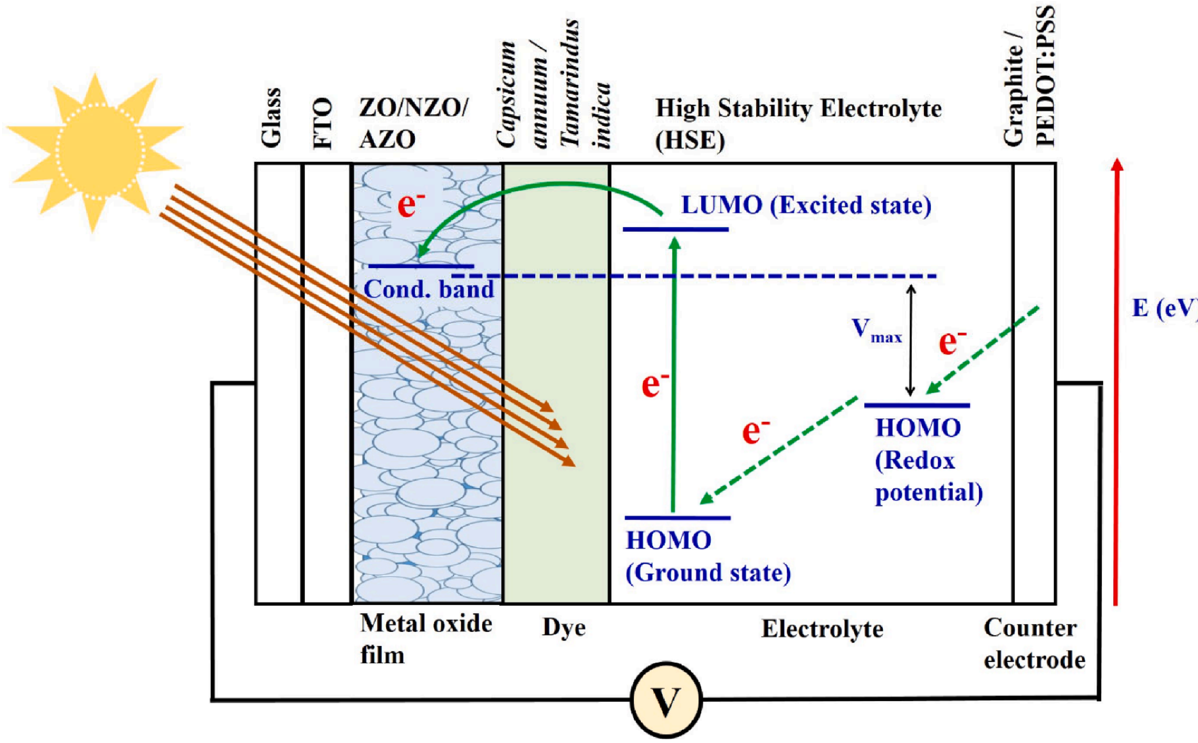

Fig. 1. Schematic illustration of the functioning of a DSSC.

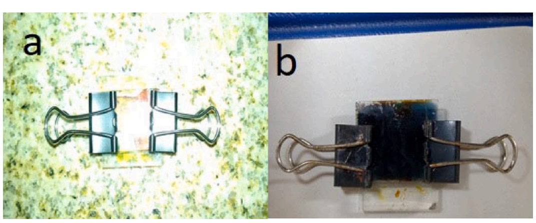

Fig. 2. Real photograph of assembled DSSCs: graphite (a) and PEDOT:PSS (b) as the counter electrode.

2011).

Generally, transition metal compounds (ruthenium polypyridyl complexes) are used as photosensitizers due to their charge-transfer absorption in the visible range. Natural dyes are alternatives to metal-based dyes like ruthenium (Ru); N719, N3, etc. Ruthenium-based dyes are expensive, have a complex structure, and have environmental concerns. Natural dyes can be another option and are considered a part of current investigations of DSSCs (Zhou et al., 2011). Dyes play a key role in harvesting sunlight and transforming solar energy into electric energy (Grätzel, 2003). Natural dyes have distinct features: economically inexpensive, easy preparation, nontoxicity, complete biodegradability, eco-friendly, and wide availability. Various natural dyes can be extracted and prepared from different plants, flowers, fruits, seeds, and leaves (El-Agez et al., 2014; Ito et al., 2010; Chou et al., 2007). Plants' stems, leaves, roots, latex, seed, fruit, etc., can all be the source of natural dyes in the form of extracts (Hao et al., 2006). These extracts are also being used as a capping or dispersing agent in the green synthesis of nanoparticles (Makarov et al., 2014).

There are various natural dyes extracted and prepared from different plants by easy procedures. Any sensitizer should absorb the maximum solar radiation energy necessary for improved cell conductivity. A natural sensitizer contains carboxyl and hydroxyl-based compounds needed for interfacing with the semiconducting nanolayer in the DSSCs to enhance the absorption of the electromagnetic spectrum (Richhariya et al., 2017). In nature, the dyes or pigments are there in various parts of the plants, such as seeds, flowers, fruits, leave, etc., to be used for DSSC (Shalini et al., 2015).

Due to their cost-effectiveness, abundance, chemically safe nature, and facile preparation, natural dyes are famous for the sensitization process in solar cells (Hemalatha et al., 2012). When sunlight interacts with the electronic structure of dyes (chlorophyll, carotenoid, flavonoid, and anthocyanin) having certain spectral properties, it is dispersed along with the change in its wavelength (Kumara et al., 2013). The energy requirements for exciting dye molecules, from HOMO to LUMO, by incident light, are different in chlorophyll, carotenoid, flavonoid, and anthocyanin. The minimum energy requirement is for flavonoids, and they can easily be adsorbed to the surface of semiconducting material. Therefore, these dyes interfaced with a semiconducting surface; they move an OH counter ion from the semiconducting nanomaterial; later, this OH ion combines with the proton provided by the dye (Ludin et al., 2014).

Anthocyanin dye and TiO_2 semiconducting material are employed in the DSSC, and the obtained efficiency is 0.56% (Olea et al., 1997). Using blackberry extract to sensitize the TiO_2 in a DSSC produces maximum current and overall efficiency of 4 mA and 1%, respectively (Garcia et al., 2003). No collective effects have been seen in the case of mixed dyes incorporated in the construction of DSSC having a TiO_2 layer (Calogero et al., 2010). The best performance of 1.70% is noted for the DSSC based on red turnip extract. The wild Sicilian prickly pear extract revealed a 9.4 mA/cm^2 current density and 1.26% conversion efficiency. Moreover, pomegranate extract as a dye in DSSC has also revealed an efficiency of 1.50%. Also, TiO_2 with gold NPs as Schottky barrier helps better dye-absorption in a DSSC and sufficed a 1.49% power conversion efficiency (Garcia et al., 2003). The efficiency of 1.8% is noted for Punica Grantum peel consisting of anthocyanins (Hemandez-Martinez et al., 2012). Similarly, red turnip contains Betalin dye is recognized for its photosensitization to produce 1.7% efficiency (Calogero et al., 2010).

Material-based dyes, active medium, and conjugated layers have been studied in DSSCs for their solar energy conversion potential. But the natural dyes extracted from recyclable and sustainable green

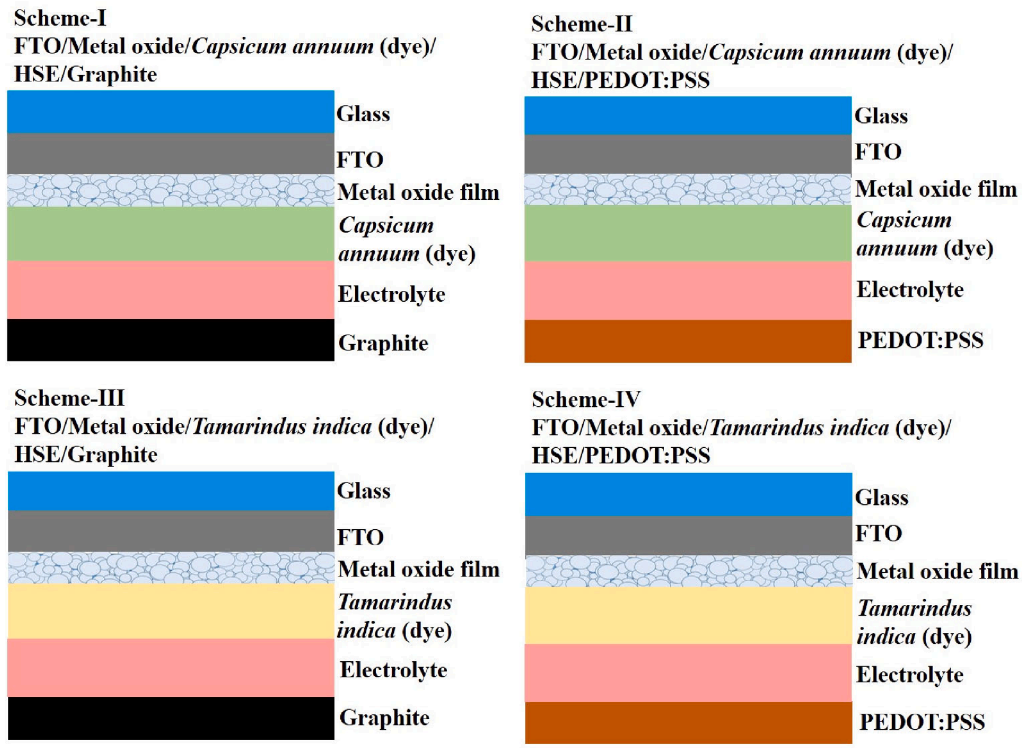

Fig. 3. Schematic representations of selected designs of DSSC in this article. Films of various materials are stacked together in four different schemes.

Table 1
List of the DSSC configurations with their names as used throughout the article.

Dye	Scheme	DSSC name	Configuration
Capsicum annuum	Scheme-I	DSSC-1	FTO/ZO/*Capsicum annuum* (dye)/ HSE/Graphite
		DSSC-2	FTO/NZO/*Capsicum annuum* (dye)/ HSE/Graphite
		DSSC-3	FTO/AZO/*Capsicum annuum* (dye)/ HSE/Graphite
	Scheme-II	DSSC-4	FTO/ZO/*Capsicum annuum* (dye)/ HSE/PEDOT:PSS
		DSSC-5	FTO/NZO/*Capsicum annuum* (dye)/ HSE/PEDOT:PSS
		DSSC-6	FTO/AZO/*Capsicum annuum* (dye)/ HSE/PEDOT:PSS
Tamarindus indica	Scheme-III	DSSC-7	FTO/ZO/*Tamarindus indica* (dye)/ HSE/Graphite
		DSSC-8	FTO/NZO/*Tamarindus indica* (dye)/ HSE/Graphite
		DSSC-9	FTO/AZO/*Tamarindus indica* (dye)/ HSE/Graphite
	Scheme-IV	DSSC-10	FTO/ZO/*Tamarindus indica* (dye)/ HSE/PEDOT:PSS
		DSSC-11	FTO/NZO/*Tamarindus indica* (dye)/ HSE/PEDOT:PSS
		DSSC-12	FTO/AZO/*Tamarindus indica* (dye)/ HSE/PEDOT:PSS

resources also need to be utilized seriously and extensively, especially from an environmental point of view. Moreover, it is well-known that different natural dyes exhibit different photosensitizing properties, and therefore, they need to be explored for their best power conversion performance. In the literature, there is no such work that has considered the natural dyes, nanomaterials, and electrodes arranged alternatively to construct DSSCs for solar energy conversion investigations. This is a novel part of this article where, dye-sensitized solar cells based on two natural dyes *Tamarindus indica* and *Capsicum annuum* extracted from their seeds, ZnO and Ni, Al-doped ZnO nanomaterials, and choices of counter electrode materials; Graphite and PEDOT:PSS [poly (3,4-ethylenedioxythiophene):poly (styrenesulfonate)] are prepared and explored for their solar energy conversion potential in the form of 12 different kinds of DSSCs. This article highlights the significance of naturally sustainable resources for solar spectrum harvesting.

2. Working of DSSC

Schematically the working of a DSSC is explained in Fig. 1, by considering the stacked layers of prepared and standard materials in this article. By nature, the materials ZnO (ZO), Ni-doped ZnO (NZO), and Al-doped ZnO (AZO) are not useful for producing photoelectrons (Sharma et al., 2018). Therefore, sensitizing dyes, *Capsicum annuum* and *Tamarindus indica* can maximize the light absorbance to enhance the photogeneration of electrons. *Capsicum annuum* or *Tamarindus indica* dye molecules in DSSC produce excited electrons when sunlight falls on its surface. The transition of electrons from the highest occupied molecular orbital (HOMO) to the lowest unoccupied molecular orbital (LUMO). These electrons instantaneously move to the conduction band of the semiconductor interlayer (ZO, NZO, or AZO). The conduction band of the semiconducting NPs lies below the excited state of a dye. The electrons produced from the incident energy, which lies in the UV–vis region, are percolated through the nanoparticles'-based interlayer and diffuse into the conducting FTO (fluorine-doped tin oxide) connected with the external circuit. On the other side, the reduction process occurs at the counter electrode (Graphite or PEDOT:PSS); as a result, the electrolyte medium receives electrons from the coupled electric circuit.

3. Experimental procedure

3.1. Extraction of natural dye sensitizers

Natural dyes were extracted from plant seeds *Capsicum annuum* (Paprika) and *Tamarindus Indica* (Tamarind). After washing with distilled water and drying at 50 °C for 24 h, seeds were ground

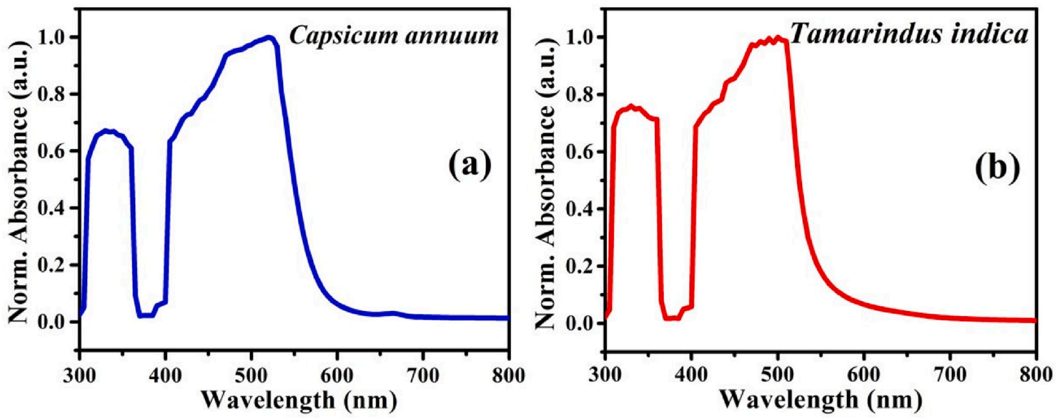

Fig. 4. The absorption spectra of natural dyes; (a) *Capsicum annuum* and (b) *Tamarindus indica*.

Table 2
UV–vis characteristics of natural dyes and prepared nanoparticles.

Natural dyes and nanomaterials	Absorption edge (nm)	Band gap energy (eV)
Capsicum annuum	525	2.36
Tamarindus indica	510	2.40
ZnO	364	3.47
Ni-doped ZnO	330	3.08
Al-doped ZnO	325	3.16

separately to obtain their powder form. One gram of powder of *Capsicum annuum* and *Tamarindus indica* extracts was added, separately, to the 10 ml ethanol and placed in the dark for one day under normal temperature and pressure. After 24 h, filtration of two solutions delivered, *Capsicum annuum* extract (CAE) and *Tamarindus indica* extract (TIE) of natural dyes, which were concentrated by heating at 40 °C to a final volume of 5 ml (Tennakone et al., 1997). Dye solutions were kept protected from direct sunlight exposure until their use in cell fabrication.

3.2. Synthesis of ZnO nanoparticles

ZnO (ZO) nanoparticles were prepared by the sol–gel technique (Znaidi, 2010). Sodium hydroxide (NaOH) of 1.0 M (4 gm) was dissolved in distilled water and heated up to 90 °C under constant stirring. Solutions of 0.5 M (6.81 gm) of $ZnCl_2$ and 0.5 M (14.87 gm) of $Zn(NO_3)_2{\cdot}6H_2O$ were slowly added through dripping for 40–100 min into the solution of NaOH after achieving the required temperature of the reactor. Immediately, the precipitates of zinc oxide (ZnO), a gel-type, were formed as indicated by the color change of the solution from transparent to white. The agitation period of the reaction was 150 min approximately. Finally, after repeated washing with distilled water, filtering, and vacuum drying at 80 °C, the ZnO material was abraded into a fine powder.

3.3. Synthesis of Ni-doped ZnO (NZO) nanoparticles

Ni-doped ZnO (NZO) nanoparticles were produced employing a hydrothermal approach (Rana et al., 2016). Solution-A of 1.0 M (8.83 gm) of zinc acetate dihydrate ($Zn(CH_3COO)_2{\cdot}2H_2O$) was prepared by dissolving in a distilled water and ethanol mixture of 40:10 ratio. Another solution-B was prepared by dissolving 0.1 M (1.163 gm) nickel nitrate hexahydrate ($Ni(NO_3)_2{\cdot}6H_2O$) in distilled water and ethanol of 40:10 ratio. Solution-A and solution-B were mixed by dripping to form solution-C. Milky-colored precipitates of zinc acetate appeared when 10 ml ammonia solution was added dropwise in solution C with vigorous stirring. 1.0 M buffer solution of sodium hydroxide (NaOH) was prepared separately and added into solution-C dropwise until the turbidity appeared. The resultant precipitates were filtered and washed several times with distilled water. Afterward, the obtained substance was dried in a vacuum oven at 70 °C for 90 min and then dried at 500 °C for 1 h in a muffle furnace to get a purified nanopowder of Ni-doped ZnO (NZO). Finally, the powder was pestled before further use.

3.4. Synthesis of Al-doped ZnO (AZO) nanoparticles

Aluminum-doped zinc oxide (AZO) nanoparticles were prepared via the sol–gel method (Khan et al., 2013). Starting with the preparation of a solution of 1.0 M of zinc acetate dihydrate ($Zn(CH_3COO_2)_2{\cdot}2H_2O$) by dissolving an amount of 10.977 gm in 50 ml of distilled water. After initial stirring and heating at 80 °C for 15 min, 0.5 at% (6.17 gm) of aluminum sulfate ($Al_2\ (SO_4)_3{\cdot}18H_2O$) was added to the zinc acetate solution. After vigorous stirring at 80 °C, the solution transformed into a gel-like material. Later, by mixing citric acid ($C_6H_8O_7$) dropwise to set the pH of the solution at 1.5, the ammonia solution (10 ml) was added. Finally, centrifugation of gel-like solution at 6000 rpm sufficed the required Al-doped ZnO nanoparticles. The obtained material was first vacuum dried at 100 °C, then annealed at 500 °C for 3 h. After the heat treatments, the AZO material was ground to achieve a dark brown fine powder.

3.5. Assembling of DSSCs

Dye-sensitized solar cells were assembled using FTO conductive glass sheets, procured from Sigma Aldrich, Product of USA, of area 2.4 × 2.4 cm^2 with a sheet resistance of 15 Ω/cm^2 and transmission > 80 %. Cleaning agents, acetone, ethanol and isopropanol in an ultrasonic bath were used after one another to clean the glass sheets, followed by distilled water rinsing to get rid of residuals. For the dimensions of the ZnO film, plastic adhesive tape was applied to the glass sheet. A homogenous ZnO paste was prepared by grinding 50 mg of ZnO nanoparticles in ethanol in a mortar for 5 min (Pervez et al., 2018). ZnO thin film was developed on FTO glass by the doctor blade method. Later it was dried by heating at 60 °C for 20 min. During cooling to room temperature, the film was dipped, for 24 h, in an alcoholic solution of *Capsicum annuum* and *Tamarindus Indica* (as natural dye sensitizers). Molecules of these dyes were adsorbed on the surface of porous ZnO film. Similarly, the same route was adopted for achieving Ni-doped ZnO and Al-doped zinc oxide films on conducting glass.

Two different types of counter electrodes were prepared for dye-sensitized solar cells. The counter electrodes, graphite (prepared by a lead pencil) and PEDOT:PSS materials were considered. The electrode materials were coated on conducting FTO (fluorine-doped tin oxide) separately by a spin coating method. Both electrode materials were provided a gentle heat treatment (at 40 °C on a hot plate) to homogenize the films (Yue et al., 2013). Final photovoltaic devices as the integrated cells are shown in Fig. 2. For the assembling of the dye-sensitized solar

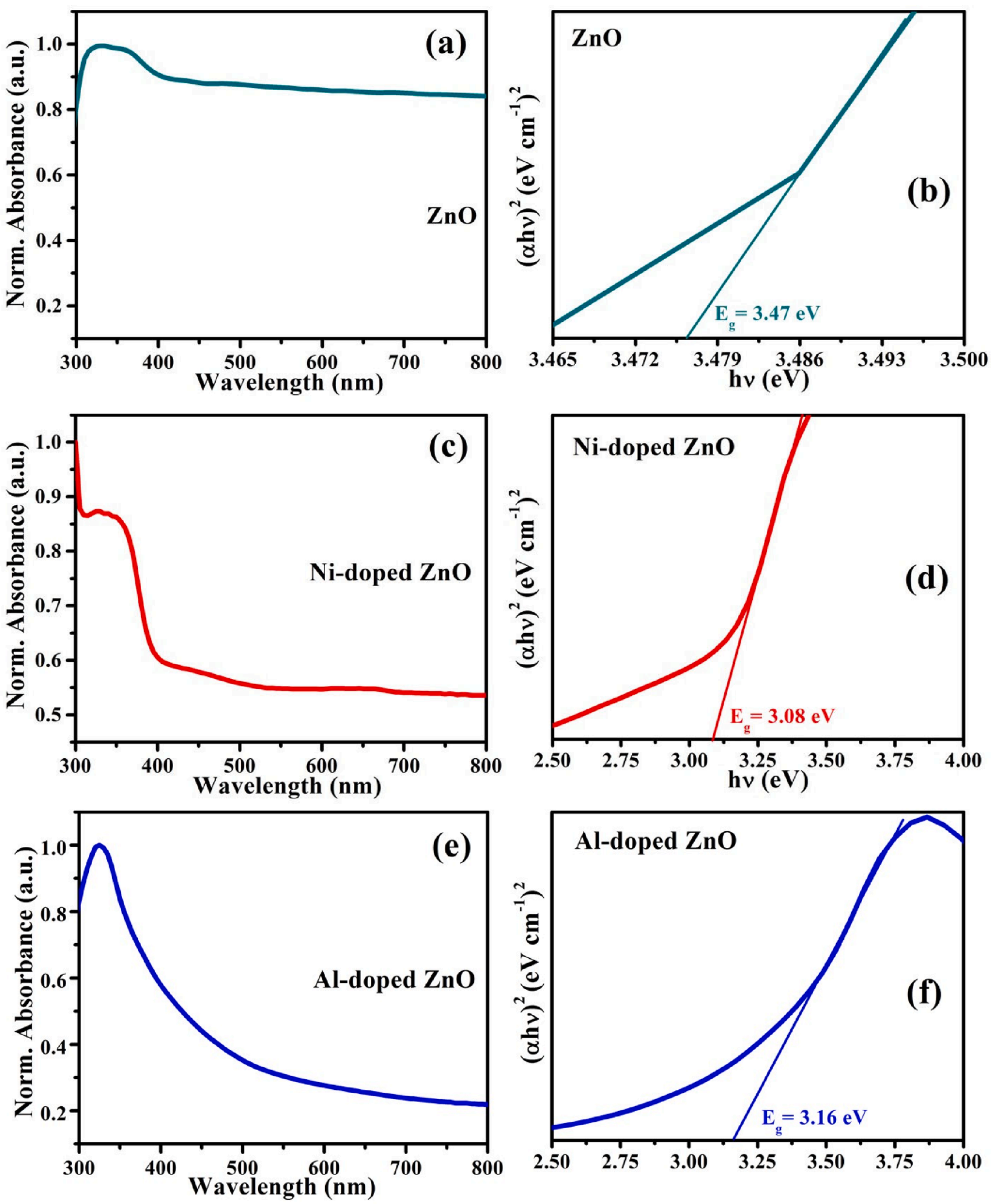

Fig. 5. UV–vis absorption spectra of ZnO nanoparticles (a), Ni-doped ZnO nanoparticles (c), and Al-doped ZnO nanoparticles (c).

cell, an electrolyte was applied between the sensitized nanoparticle layer (as a photoanode) and graphite/PEDOT:PSS (as a counter cathode) (Wei et al., 2011). The high stability electrolyte (HSE), procured from Solaronix, was used as a redox mediator (non-volatile HSE). Real photographs of the assembled DSSCs are shown in Fig. 2. All the interlayers with outer electrodes are clipped together.

3.6. Configurations of DSSCs

To evaluate the efficiency of DSSCs in this article following different parts of each cell were arranged alternatively to achieve 12 different possibilities.

1. Capsicum annuum or Tamarindus indica as a sensitizing dye
2. ZO, NZO, or AZO as a semiconductor interlayer
3. Graphite or PEDOT:PSS as an electrode

Whereas the glass, FTO and high stability electrolyte (HSE) remained unchanged in all four schemes. Where all four schemes were considered by varying dye, interlayer and electrode. The selected DSSCs are schematically illustrated in Fig. 3. For all these opted DSSCs, the choice of *Capsicum annuum* or *Tamarindus indica* allowed us to evaluate its effect on the efficiency of the final device. The names of all DSSCs and materials stacked together are listed in Table 1.

3.7. Photovoltaic measurements of DSSCs

For each configured DSSC, J-V measurements were recorded to determine the respective power conversion efficiency. Measurements were done at a computer-controlled source meter (Keithley 2400) under a solar simulator (Oriel Sol3A, Newport). Observations were noted for the sweeping voltage window 0–1.0 V at 0.1 V/s. The power conversion efficiency $\eta = \frac{V_{OC} \times J_{SC} \times FF}{P_{in}}$ of prepared DSSCs was obtained (Hou et al., 2013) from the J-V curves, where V_{oc} is open-circuit voltage and J_{sc}

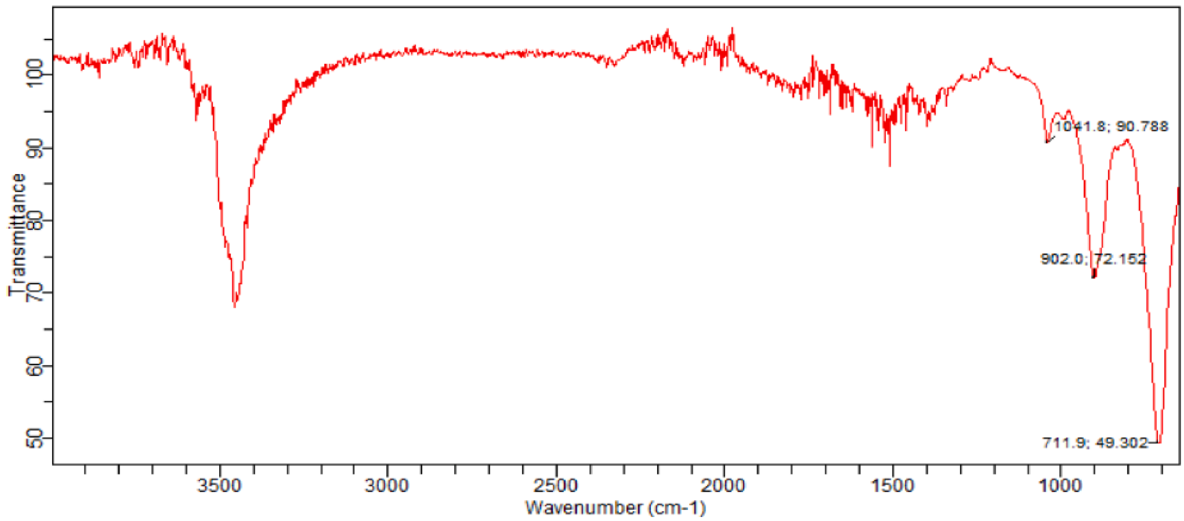

Fig. 6. FTIR spectrum of zinc oxide (ZnO) nanoparticles.

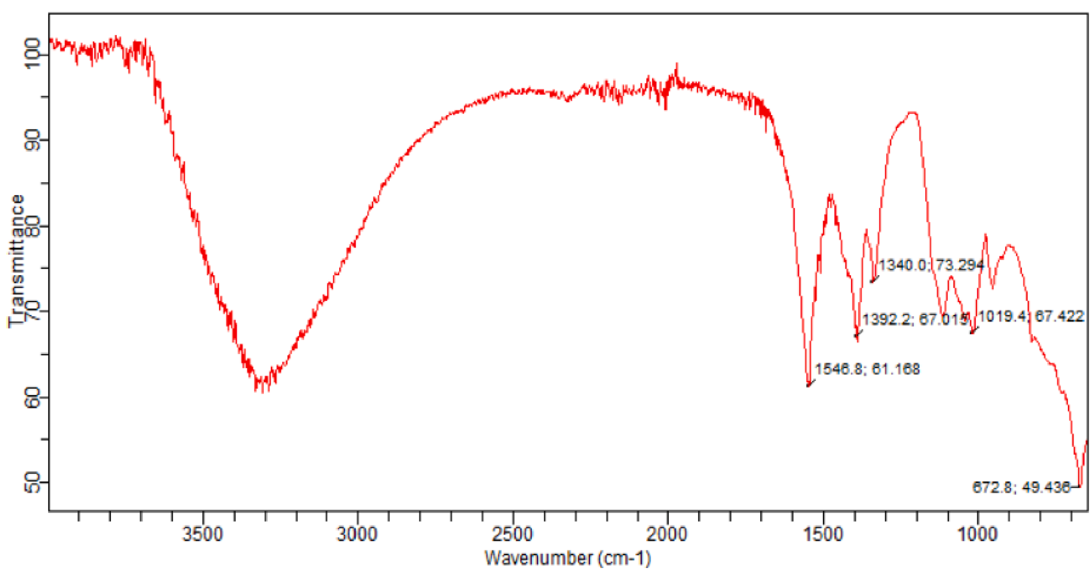

Fig. 7. FTIR spectrum of nickel-doped zinc oxide (NZO) nanoparticles.

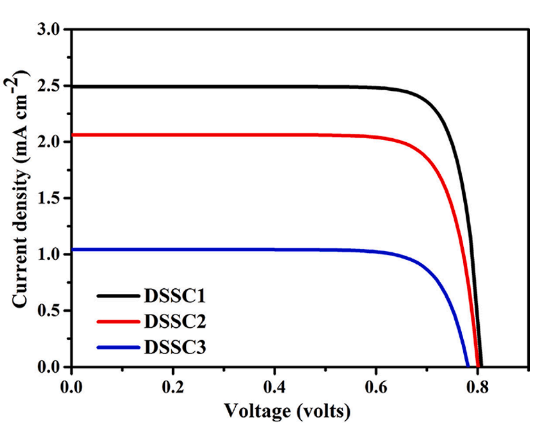

Fig. 8. J-V curves of DSSC1: FTO/ZO/*Capsicum annuum* (dye)/HSE/Graphite, DSSC2: FTO/NZO/*Capsicum annuum* (dye)/HSE/Graphite, and DSSC3: FTO/AZO/*Capsicum annuum* (dye)/HSE/Graphite.

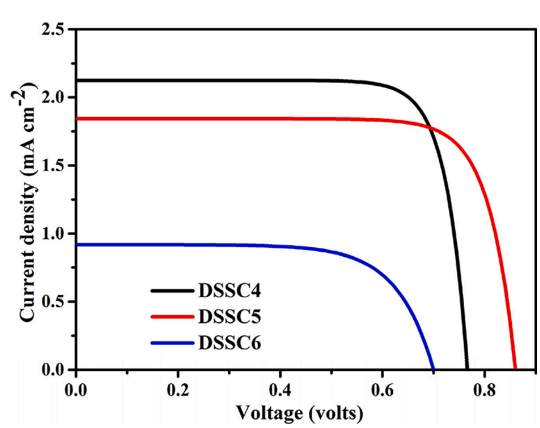

Fig. 9. J-V curves of DSSC4: FTO/ZO/*Capsicum annuum* (dye)/HSE/PEDOT:PSS, DSSC5: FTO/NZO/*Capsicum annuum* (dye)/HSE/PEDOT:PSS, and DSSC6: FTO/AZO/*Capsicum annuum* (dye)/HSE/PEDOT:PSS.

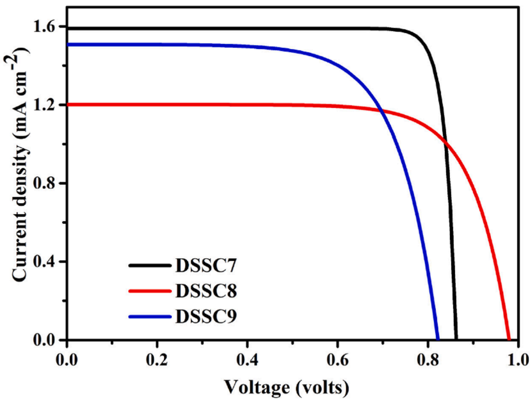

Fig. 10. J-V curves of DSSC7: FTO/ZO/*Tamarindus indica* (dye)/HSE/Graphite, DSSC8: FTO/NZO/*Tamarindus indica* (dye)/HSE/Graphite, and DSSC9: FTO/AZO/*Tamarindus indica* (dye)/HSE/Graphite.

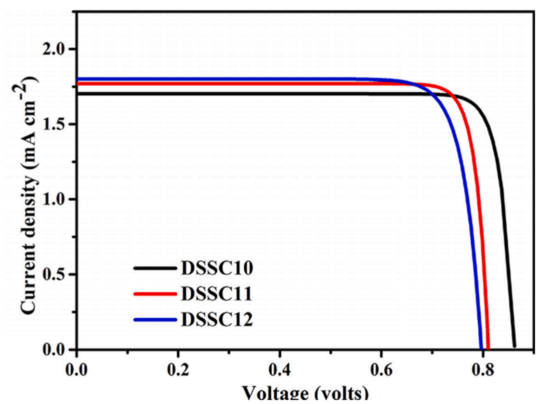

Fig. 11. J-V curves of DSSC10: FTO/ZO/*Tamarindus indica* (dye)/HSE/PEDOT:PSS, DSSC11: FTO/NZO/*Tamarindus indica* (dye)/HSE/PEDOT:PSS, and DSSC12: FTO/AZO/*Tamarindus indica* (dye)/HSE/PEDOT:PSS.

(short circuit photocurrent density. The power of incident light per unit area, P_{in}, was adjusted at 100 W/m^2. Current density J_{sc} in mA/cm^2 and fill factor FF, defined as $FF = \frac{V_{max}\,J_{max}}{V_{OC}\,J_{SC}}$, were considered for the power conversion efficiency calculations. V_{max} and J_{max} were the maximum voltage and maximum photocurrent density, respectively.

4. Results and discussion

4.1. UV–vis spectroscopy

One of the ultimate goals in solar cell science and technologies is to capture the maximum spectrum of light by reducing the band gap energy of the active medium. The active/conjugated medium may be a single substance or a combination of two or more materials. In the present case, *Capsicum annuum* and *Tamarindus indica* are playing their role as light-absorbing mediums. Due to low band gap energies, these dyes are favorable for fabricating dye-sensitized solar cells (DSSCs) as an active layer material. Band gap energy calculations are done by the Tauc's relation, $\alpha h\nu = C(h\nu - E_g)^n$, where α is absorbance, C is a constant, and n is to identify the direct and indirect band gap transition. By plotting $(\alpha h\nu)^2$ against incoming photon energy, $E = h\nu$ suffices the desired band gap energy.

UV–vis absorption spectra of natural dyes; *Capsicum annuum* and *Tamarindus indica* are shown in Fig. 4. *Capsicum annuum* and *Tamarindus indica* seed extracts have characteristic absorption edges of 510 nm and 525 nm, respectively. According to Tauc's plot, the band gap energies are 2.36 eV of *Capsicum annuum* and 2.40 eV of *Tamarindus indica*. For *Tamarindus indica*, the UV–vis absorption spectrum is analogous to absorption peaks in the ultraviolet and blue-green regions. The analogous absorption peaks of the *Capsicum annuum* exist in the UV and blue regions. The absorption edge and band gap energies of considered natural dyes are listed in Table 2.

The UV–vis absorption spectrum of synthesized zinc oxide (ZnO) nanoparticles is shown in Fig. 5(a). The strong absorption is observed at 364 nm. Whereas the band gap energy of nanoparticles is calculated as 3.47 eV.

The UV–vis response of nickel-doped zinc oxide (NZO) nanoparticles and aluminum-doped zinc oxide (AZO) nanoparticles are shown in Fig. 5 (c,e). The absorption edge is shifted to the lower energies due to the incorporation of Ni or Al atoms inside the ZnO matrix separately (Yue et al., 2013). In the case of Ni doping in ZnO, the band gap is shifted to 3.08 eV from 3.47 eV, as shown in Fig. 5(d). The band gap energy of 3.47 eV of pure ZnO reduces to the band gap energy of 3.16 eV by Al-doping in ZnO. The annealing of specimens was done to improve the electro-optical characteristics of the nanoparticles (Jin et al., 2000). The band gap energies of undoped and co-doped ZnO nanoparticles are listed in Table 2.

4.2. X-ray diffraction

X-ray diffraction results indicated the desired crystalline nature of the prepared nanomaterials.

4.3. FTIR analysis

In the FTIR spectrum of ZnO NPs, shown in Fig. 6, a broad peak at 3460 cm^{-1} indicates the O–H stretching and bending modes associated with water absorbed at the surface of metal oxide nanoparticles. Two stretching modes are present at 711.9 cm^{-1} and 902.0 cm^{-1}, indicating the Zn–O lattice. Another peak around 1041 cm^{-1} is attributed to the C–N stretching mode (Music et al., 2002).

FTIR spectrum of Ni-doped ZnO nanoparticles is presented in Fig. 7. The characteristic peak of stretching Ni-Zn-O asymmetric vibrations exists at 673 cm^{-1}. The stretching O–H vibrations at 1110 cm^{-1} and 3335 cm^{-1} are associated with the hydroxyl group. The IR peaks at 1340 cm^{-1} and 1546 cm^{-1} are attributed to C=O symmetric and asymmetric stretching modes, i.e., the carbonyl group exists on the ZnO surface due to absorption. C–H stretching mode is indicated at 1019 cm^{-1} (Raja et al., 2014; Cong et al., 2005).

4.4. J-V measurements

The J-V curves of all DSSC configurations for *Capsicum annuum* and *Tamarindus indica* dyes have been plotted in Figs. 8-9, and Figs. 10-11, respectively. The characteristics parameters, derived from the J-V curves, are plotted in Fig. 12 for all twelve DSSC configurations.

Fig. 8 includes the J-V plots of DSSCs arranged by considering different metal oxide NPs while keeping other layers of FTO, *Capsicum annuum* dye, HSE, and graphite electrodes fixed. Compared to Fig. 8, J-V plots in Fig. 9 are obtained by selecting different metal oxide NPs and the PEDOT:PSS electrode instead of graphite. In contrast, the natural dye *Capsicum annuum* remains the same. So this will lead to six different schemes to study the DSSCs based on *Capsicum annuum* as a natural dye for solar energy conversion. Following the pattern of DSSCs, as explained above, J-V curves are measured for the other six DSSC designs by only replacing *Capsicum annuum* with *Tamarindus indica* dye. All outer and intermediate layers of metal oxide NPs, electrolyte, and electrode materials remain the same in DSSCs settings.

In Fig. 12(a), the maximum open-circuit voltage (V_{oc}) of 0.98 V is calculated for DSSC-8 (FTO/NZO/*Tamarindus indica* (dye)/HSE/Graphite), whereas the minimum V_{oc} of 0.69 V is noted for DSS-6 (FTO/AZO/*Capsicum annuum* (dye)/HSE/PEDOT:PSS). In Fig. 12(c), the

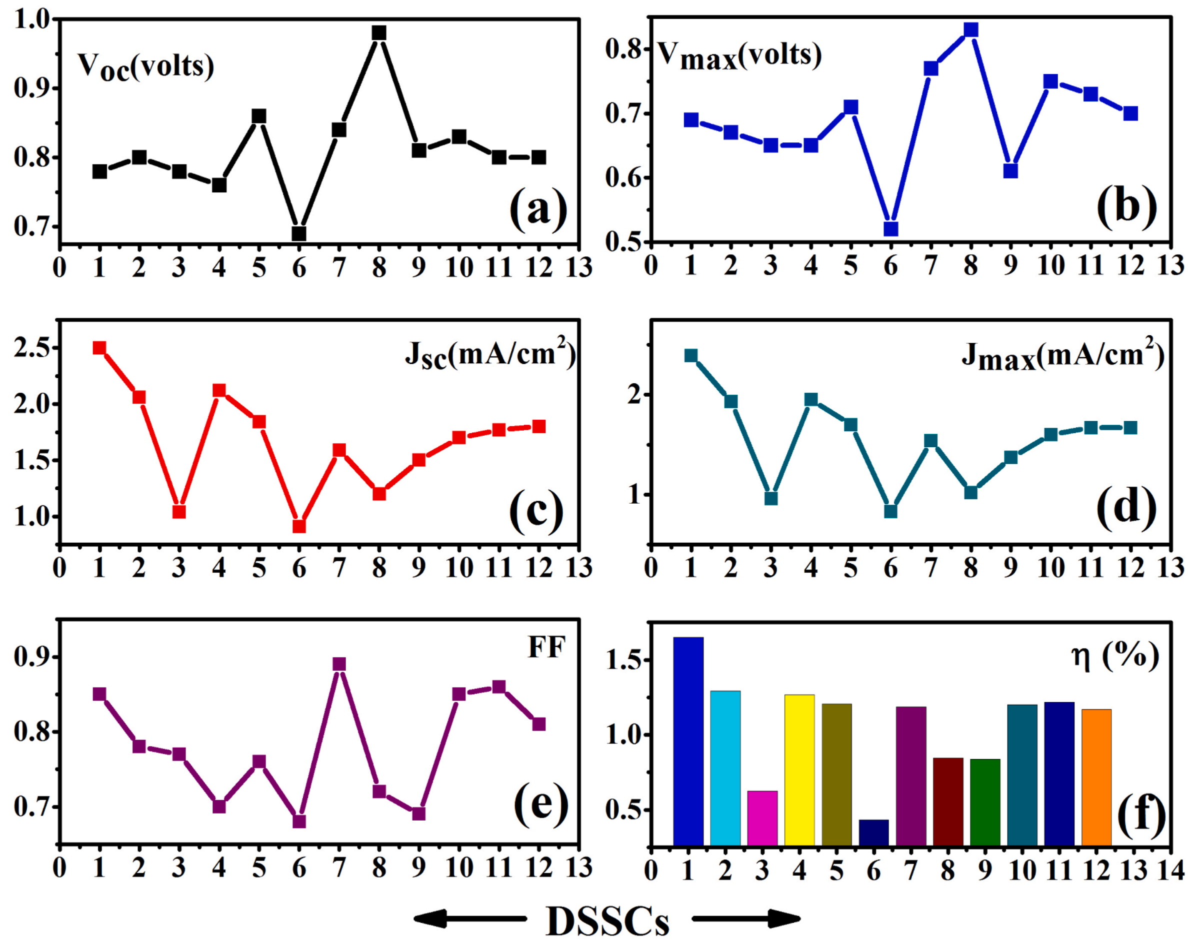

Fig. 12. Open-circuit voltage (a), maximum voltage (b), short circuit current density (c), maximum current density (d), fill factor (e), and power conversion efficiency (f) of all 12 DSSCs.

Table 3
Power conversion efficiencies and other parameters of all selected DSSCs.

Dye	Schemes	DSSC name	Configuration	V_{oc} (volts)	J_{sc} (mA /cm^2)	FF	η (%)
Capsicum annuum	Scheme-I	DSSC-1	FTO/ZO/*Capsicum annuum* (dye)/HSE/Graphite	0.78	2.5	0.85	1.65
		DSSC-2	FTO/NZO/*Capsicum annuum* (dye)/HSE/Graphite	0.8	2.06	0.78	1.29
		DSSC-3	FTO/AZO/*Capsicum annuum* (dye)/HSE/Graphite	0.78	1.04	0.77	0.62
	Scheme-II	DSSC-4	FTO/ZO/*Capsicum annuum* (dye)/HSE/PEDOT:PSS	0.76	2.12	0.7	1.27
		DSSC-5	FTO/NZO/*Capsicum annuum* (dye)/HSE/PEDOT:PSS	0.86	1.84	0.76	1.21
		DSSC-6	FTO/AZO/*Capsicum annuum* (dye)/HSE/PEDOT:PSS	0.69	0.91	0.68	0.43
Tamarindus indica	Scheme-III	DSSC-7	FTO/ZO/*Tamarindus indica* (dye)/HSE/Graphite	0.84	1.59	0.89	1.19
		DSSC-8	FTO/NZO/*Tamarindus indica* (dye)/HSE/Graphite	0.98	1.2	0.72	0.84
		DSSC-9	FTO/AZO/*Tamarindus indica* (dye)/HSE/Graphite	0.81	1.5	0.69	0.84
	Scheme-IV	DSSC-10	FTO/ZO/*Tamarindus indica* (dye)/HSE/PEDOT:PSS	0.83	1.7	0.85	1.2
		DSSC-11	FTO/NZO/*Tamarindus indica* (dye)/HSE/PEDOT:PSS	0.8	1.77	0.86	1.22
		DSSC-12	FTO/AZO/*Tamarindus indica* (dye)/HSE/PEDOT:PSS	0.8	1.8	0.81	1.17

maximum short circuit current density (J_{sc}) of 2.5 mA/cm^2 is obtained in the case of DSSC-1 (FTO/ZO/*Capsicum annuum* (dye)/HSE/Graphite), which also shows maximum power conversion efficiency. On the other hand, a minimum short circuit current density (J_{sc}) of 0.91 mA/cm^2 is measured for DSSC-6 (FTO/AZO/*Capsicum annuum* (dye)/HSE/PEDOT:PSS), which also exhibits minimum efficiency as the final device. In Fig. 12(c), the fill factor (FF) is maximum, that is 0.89, in the case of DSSC-7 (FTO/ZO/*Tamarindus indica* (dye)/HSE/Graphite), whereas it is 0.68 minimum FF for the DSSC-6 (FTO/AZO/*Capsicum annuum* (dye)/HSE/PEDOT:PSS). DSSC-7 is among the DSSC configurations having higher power conversion efficiencies than the DSSC-6.

According to Table 3, DSSC-1: FTO/ZO/*Capsicum annuum* (dye)/HSE/Graphite shows maximum efficiency compared to all other arrangments. The efficiency is decreased by 28% in DSSC-7, where the natural dye *Capsicum annuum* is replaced by *Tamarindus indica*. Similarly, the efficiency of DSSC-2 is larger than the DSSC-8, where the ZnO layer replaces by the Ni-doped ZnO layer, while the *Capsicum annuum* replaces by *Tamarindus indica*. But in the case of DSSC-3, the efficiency is smaller than the DSSC-9 having an Al-doped ZnO layer in both configurations while the *Capsicum annuum* is replaced by *Tamarindus indica*.

In scheme-II and scheme-IV, the DSSCs performance is measured using PEDOT:PSS as an electrode material. The efficiency of all the cells is approximately the same except for DSSC-6 and DSSC-12. The efficiencies of DSSC-1 and DSSC-4 are compared to see the effect of

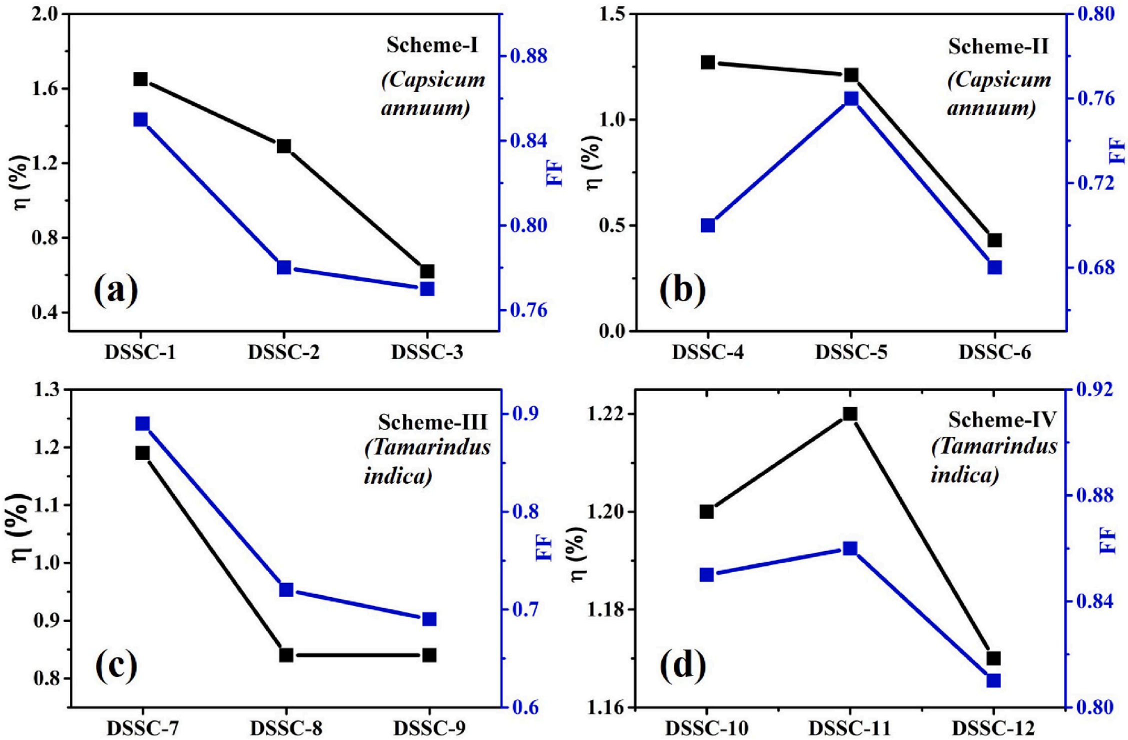

Fig. 13. Comparison of η and FF of all four sets of the DSSC schemes.

electrode material. The efficiency dropped by 23% from DSSC with PEDOT:PSS as an electrode layer compared to the DSSC with graphite as an electrode. The efficiency of DSSC with ZnO is superior to the Al or Ni-doped ZnO nanomaterial layer with alternatively considered natural dyes. The DSSCs with *Capsicum annuum* as a sensitizing dye are more efficient in all configurations than the *Tamarindus indica*. Overall better photon absorption and performance point of view, the DSSC-1 with the configuration, FTO/ZO/*Capsicum annuum* (dye)/HSE/Graphite is at the top among all twelve DSSCs. Further, in DSSC-1, not only a dye but also the ZnO NPs layer and electrode material play their role during the photon-energy conversion process. The efficiencies of all twelve DSSC arrangements are sown in Fig. 12(f).

In configurations of DSSCs of schemes I and III, there is a trend of a gradual decrease in η and FF when replacing ZnO with Ni-doped ZnO and Al-doped ZnO films, as shown in Fig. 13(a,c). But in the case of DSSCs of schemes II, the η decreases continuously while FF first increases and then decreases when ZnO film is exchanged by Ni-doped ZnO and then by Al-doped ZnO films (Fig. 13(b). For DSSCs of scheme IV, both η and FF first increase and then decrease when considering the Ni-doped ZnO and then Al-doped ZnO films instead of ZnO Fig. 13(d).

Anthocyanin is the pigment present in the seed extracts of *Capsicum annuum* (Amogne et al., 2020) and *Tamarindus indica* (Mayavel et al., 2012) responsible for sensitizing the ZnO and co-doped ZnO films in the selected DSSC configurations. Anthocyanin in *Capsicum annuum* and *Tamarindus indica* can develop bonds with the metal ions through carbonyl and hydroxyl groups (Norasikin et al., 2014) necessary for solar energy conversion. Along with the production of excitons, these dyes also change the absorption maxima by the adsorption process that occurs at the surface of ZnO, Al, or Ni-doped ZnO responsible for charge transportation. Further, the carbonyl and hydroxyl groups present in the anthocyanin molecules of *Capsicum annuum* and *Tamarindus* develop different interfacial interactions with the prepared metal oxide layers. Also, it is important to mention that the conduction bands of ZnO and co-doped ZnO are different; therefore, the charge flow is variable through them. As a result, random transportation trends are observed in different DSSCs.

5. Conclusion

Natural dyes *Capsicum annuum* and *Tamarindus indica* have been investigated for their role as an active medium for light absorption in DSSCs with the choices of metal oxide interlayers and electrode materials. Various DSSC configurations have been achieved by combining a dye from *Capsicum annuum* and *Tamarindus indica*, nanoparticle layers from ZO, NZO, and AZO, and electrode material from Graphite and PEDOT:PSS. Other necessary layers such as FTO and HSE have been provided in all selected DSSC schemes. Results show that the maximum power conversion efficiency of 1.65% has been found in the case of DSSC configured as FTO/ZO/*Capsicum annuum* (dye)/HSE/Graphite. Most of the DSSCs with ZO as a transport layer reveal better efficiency. Also, it has been seen that the efficiency varies by only switching the electrode material. In general, the effect of *Capsicum annuum* or *Tamarindus* combined with the ZO, AZO or NZO suffices the arbitrary conditions for each configured DSSC for its operation with a certain efficiency.

Availability of data and materials

The raw/processed data required to reproduce these findings cannot be shared as the data also forms part of an ongoing study.

CRediT authorship contribution statement

Nasim Sarwar: Methodology, Formal analysis, Writing – original draft. **Monas Shahzad:** Conceptualization, Formal analysis, Writing – review & editing. **Rabia Ghaffar:** Formal analysis, Writing – review & editing. **Khalid Javed:** . **Mahroze Munam:** Formal analysis. **Aneel Pervez:** . **Abdul Ghaffar:** Conceptualization, Formal analysis, Writing – review & editing.

Declaration of Competing Interest

The authors declare that they have no known competing financial interests or personal relationships that could have appeared to influence the work reported in this paper.

Acknowledgment

Not considered.

References

Shalini, S., Prabhu, R.B., Prasanna, S., Mallick, T.K., Senthilarasu, S., 2015. Review on natural dye sensitized solar cells: operation, materials and methods. Renew. Sustain. Energy Rev. 51, 1306–1325.

El-Agez, T.M., Taya, S.A., Elrefi, K.S., Abdel-Latif, M.S., 2014. Dye sensitized solar cells using some organic dyes as photosensitizers. Opt. Appl. 44, 345–351.

O'Regan, B., Grätzel, M., 1991. A low-cost high-efficiency solar cell based on dye-sensitized colloidal TiO2 films. Nature 353, 737–740.

Grätzel, M., 2001. Photoelectrochemical cells. Nature 414, 332–337.

Banerjee, A.N., 2011. The design, fabrication, and photocatalytic utility of nanostructured semiconductors: focus on TiO_2-based nanostructures. Nanotechnol. Sci. Appl. 4, 35–65.

Bazargan, M.H., Byranvand, M., Kharat, A.N., Fatholahi, L., 2011. Natural pomegranate juice as photosensitizers for dye-sensitized solar cell (DSSC). Optoelectron. Adv. Mater. – Rapid Commun. 5, 360–362.

Nukunudompanich, M., Chuangchote, S., Okamoto, Y., Shinoda, Y., Suzuki, Y., 2015. TiO_2 nanorods and semi-nanotubes prepared from anodic aluminum oxide template and their applications as photoelectrodes in dye-sensitized solar cells. J. Ceram. Soc. Jpn. 123, 428–432.

Ariyasinghe, D., Bandara, H., Rajapakse, R., Murakami, K., Shimomura, M., 2013. Improved performance of dye-sensitized solar cells using a diethyldithiocarbamate-modified TiO_2 surface, Journal of Nanomaterials. J. Nanomater. 258581, 6.

Xu, S., Zhou, C., Yang, Y., Hu, H., Sebo, B., Chen, B., Tai, Q., Zhao, X., 2011. Effects of ethanol on optimizing porous films of dye-sensitized solar cells. Energy Fuels 25, 1168–1172.

Zhou, H., Wu, L., Gao, Y., Ma, T., 2011. Dye-sensitized solar cells using 20 natural dyes as sensitizers. J. Photochem. Photobiol. 219 (2), 188–194.

Grätzel, M., 2003. Dye-sensitized solar cells. J. Photochem. Photobiol. C: Photochem. Reviews 4 (1), 145–153.

Ito, S., Saitou, T., Imahori, H., Ueharad, H., Hasega-wad, N., 2010. Fabrication of dye-sensitized solar cells using natural dye for food pigment: monascus yellow. Energ. Environ. Sci. 3 (2), 905–909.

Chou, T., Zhang, Q., Cao, G., 2007. Effects of dye loading conditions on the energy conversion efficiency of ZnO and TiO_2 dye-sensitized solar cells. J. Phys. Chem. C 111 (50), 18804–18811.

Hao, S., Wu, J., Huang, Y., Lin, J., 2006. Natural dyes as photosensitizers for dye-sensitized solar cell. Sol. Energy 80 (2), 209–214.

Makarov, V.V., Love, A.J., Sinitsyna, O.V., Makarova, S.S., Yaminsky, I.V., Taliansky, M. E., Kalinina, N.O., 2014. "Green" nanotechnologies: synthesis of metal nanoparticles using plants. Acta Nat 6, 35–44.

Richhariya, G., Kumar, A., Tekasakul, P., Gupta, B., 2017. Natural dyes for dye sensitized solar cell: a review. Renew. Sustain. Energy Rev. 69, 705–718.

Hemalatha, K.V., Karthick, S.N., Justin, R.C., Hong, N.Y., Kim, S.K., Kim, H.J., 2012. Performance of *Kerria japonica* and *Rosa chinensis* flower dyes as sensitizers for dye-sensitized solar cells. Spectrochim. Acta, Part A: Mol. Biomol. Spectrosc. 96, 305–309.

Kumara, N.T.R.N., Ekanayake, P., Lim, A., Liew, L.Y.C., Iskandar, M., Ming, L.C., Senadeera, G.K.R., 2013. Layered co-sensitization for enhancement of conversion efficiency of natural dye sensitized solar cells. J. Alloys Compd. 581, 186–191.

Ludin, N.A., Al-Alwani Mahmoud, A.M., Mohamad, A.B., Kadhum, A.H., Sopian, K., Abdul Karim, N.S., 2014. Review on the development of natural dye photosensitizer for dye sensitized solar cells. Rene. Sustain. Energy Rev. 31, 386–396.

Olea, A., Ponce, G., Sebastian, P.J., 1997. Electron transfer via organic dyes for solar conversion. J. Sol. Energy Mater. Sol. Cells 59, 137–143.

Garcia, C.G., Polo, A.S., Lha, N.Y.M., 2003. Fruit extracts and ruthenium polypyridinic dyes for sensitization of TiO_2 in photo electrochemical solar cells. J. Photochem. Photobiol. 160, 87–91.

Calogero, G., Marco, G.D., Cazzanti, S., Caramori, S., Argazzi, R., Carlo, A.D., Bignozzi, C. A., 2010. Efficient dye-sensitized solar cells using red turnip and purple wild Sicilian prickly pear fruits. Int. J. Mol. Sci. 11, 254–267.

Hemandez-Martinez, A.R., Vargas, S., Estevez, M., Rodriguez, R., 2012. Natural pigment based dye-sensitized solar cells. In: First International Congress on Instrumentation and Applied Sciences, vol. 10, pp. 1–15.

Tennakone, K., Kumara, A.K., Jayantha, K.W., Sirimanne, P.M., 1997. Nanoporous TiO_2 photoanode sensitized with the flower pigment cya-niding. J. Photochem. Photobiol. 108 (2), 193–198.

Znaidi, L., 2010. Sol-gel-deposited ZnO thin films: a review. Mater. Sci. Eng. B 174 (1–3), 18–30.

Rana, A.K., Bankar, P., Kumar, Y., More, M.A., Late, D.J., Shirage, P.M., 2016. Synthesis of Ni-doped ZnO nanostructures by low-temperature wet chemical method and their enhanced field emission properties. RSC Adv. 6 (106), 104318–104324.

Khan, W., Khan, Z.A., Saad, A.A., Shervani, S., Saleem, A., Naqvi, A.H., 2013. Synthesis and characterization of Al doped ZnO nanoparticles. Int. J. Mod. Phys. Conf. Ser. World Scientific Publishing Co. 22, 630–636.

Pervez, A., Javed, K., Iqbal, Z., Shahzad, M., Khan, U., Latif, H., Shah, S.A., Ahmad, N., 2018. Fabrication and comparison of dye sensitized solar cells by using TiO_2 and ZnO as photo electrode. Optik 182, 175–180.

Yue, G., Wu, J., Xiao, Y.M., Lin, J.M., Huang, M.L., Fan, L.Q., Yao, Y., 2013. A dye-sensitized solar cell based on PEDOT:PSS counter electrode. Chin. Sci. Bull. 58, 559–566.

Wei, Y.S., Jin, Q.Q., Ren, T.Z., 2011. Expanded graphite/pencil-lead as counter electrode for dye-sensitized solar cells. Solid State Electron. 63 (1), 76–82.

Hou, J., Guo, X., 2013. Active layer materials for organic solar cells. In: Choy, W.C.H. (Ed.), Organic Solar Cells. Green Energy and Technology Springer-Verlag, London.

Jin, Y.D., Yang, J.P., Heremans, P.L., Van der Auweraer, M., Rousseau, E., Geise, H.J., Borghs, G., 2000. Single-layer organic light-emitting diode with 2.0% external quantum efficiency prepared by spin-coating. Chem. Phys. Lett. 320 (5–6), 387–392.

Music, S., Popovic, S., Maljkovic, M., Dragcevic, D., 2002. Influence of synthesis procedure on the formation and properties of zinc oxide. J. Alloys Compd. 347, 324–332.

Raja, K., Ramesh, P.S., Geetha, D., 2014. Synthesis, structural and optical properties of ZnO and Ni-doped ZnO hexagonal nanorods by Co-precipitation method. Spectrochim. Acta Part A Mol. Biomol. Spectrosc. 120, 19–24.

Cong, C.J., Hong, J.H., Liu, Q.Y., Liao, L., Zhang, K.L., 2005. Synthesis, structure and ferromagnetic properties of Ni-doped ZnO nanoparticles. Solid State Commun. 138, 511–555.

Sharma, K., Sharma, V., Sharma, S.S., 2018. Dye-sensitized solar cells: fundamentals and current status. Nanoscale Res. Lett. 13 (1), 381.

Amogne, N.Y., Ayele, D.W., Tsigie, Y.A., 2020. Recent advances in anthocyanin dyes extracted from plants for dye sensitized solar cell. Mater. Renew. Sustain. Energy 9, 23.

Mayavel, A., Singh, B., Durai, A., Murugeasan, S., 2012. Evaluation of colour and stability of anthocyanin in red tamarind (*Tamarindus indica* L). Int. J. Adv Life Sci (IJALS) 5, 137–144.

Norasikin, A.L., Mahmoud, A.M.A., Mohamad, A.B., Kadhum, A.A.H., Sopian, K., Karim, N.S.A., 2014. Review on the development of natural dye photosensitizer for dye-sensitized solar cells. Renew. Sustain. Energy Rev. 31, 386–396.